# Comparison of Calculated and Measured Critical Flow Rates for Dragging Linear Polymer Chains through a Small Cylindrical Tube

Karl F. Freed[†] and Chi Wu[*,‡]

[†]James Franck Institute and Department of Chemistry, University of Chicago, Chicago, Illinois 60637, United States

[‡]Department of Chemistry, The Chinese University of Hong Kong, Shatin, N.T., Hong Kong, and The Hefei National Laboratory of Physical Science at Microscale, Department of Chemical Physics, The University of Science and Technology of China, Hefei, Anhui 230026, China

ABSTRACT: Using recently developed analytical Green's function/numerical inverse Laplace transform methods, we calculate the hydrodynamic drag and confinement forces on a linear Gaussian chain inside an interacting and impenetrable cylindrical tube in the free draining limit. Equating the two forces leads to an estimation of the critical (minimum) flow rate (q_c) to drag the chain through the tube. The estimated q_c is compared with our measured q_c in theta solutions as well as with our previous scaling argument for a variety of experimental conditions (solvent quality and tube radius, R). Satisfactory agreement between the calculated and observed critical flow rates reveals that the previous description by de Gennes of a linear chain confined in a tube as a series of hard spheres (blobs) significantly underestimates the hydrodynamic drag force, such that the predicted q_c for the hard sphere model is 10^2-10^3 times higher than observed. The calculations also confirm our previous scaling argument that q_c decreases with increasing R, thus departing from the hard-sphere blob prediction that q_c is independent of R. More importantly, the calculation describes how interactions with the tube walls affect chain confinement.
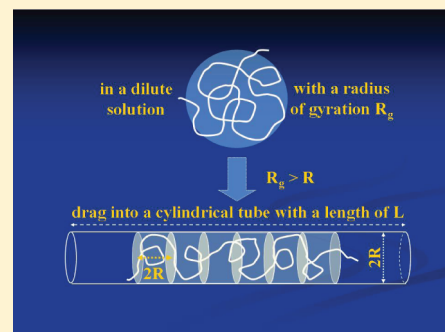
Confinement and translocation of macromolecules in and through different small geometries not only are of academic interest but also exert profound influence on many real applications, such as size exclusion chromatography, ultrafiltration, and controlled release. Moreover, biological macromolecules (proteins, DNA, and RNA) are often confined inside various structures composed of proteins, including ribosome channels, chaperons, viral capsids, and nuclear pores, to name a few. Recently, we have experimentally studied how polymer chains with different topologies are driven through a cylindrical pore by an elongation flow,[1,2] have investigated the influence of solvent quality and pore size,[3] have measured the hydrodynamic force required to pull a chain out of a core—shell polymeric micelle,[4] and have developed an effective ultrafiltration method to separate polymer chains by differences in chain topology rather than current methods that separate according to hydrodynamic sizes.[5]

Earlier theoretical treatments of geometrical confinement of polymer chains follow the pioneering 1969 studies by Casassa and Tagami[6] and Edwards and Freed,[7] who use classical eigenfunction expansion methods for solving diffusion equations, as detailed by Carslaw and Jaeger.[8] Later, using a Rouse model,[9] de Gennes[10] and Pincus[11] predict that linear polymer chains in a dilute solution can undergo a first-order coil-to-stretch transition in an elongation flow field at a critical (minimum) flow rate (q_c). This elongation thus enables the chain to pass through a much smaller cylindrical pore than its coiled size for sufficiently strong hydrodynamic drag forces, as schematically represented in Figure 1. de Gennes and Pincus assume that a confined chain may be approximated as a string of nondraining hard spheres (blobs) and

use this simple model to predict that q_c is independent of both the chain length and pore size, more specifically, that $q_c \simeq k_BT/12\pi\eta$, $k_BT/3\pi\eta$, or $k_BT/8\eta$, depending on whether each small confined space occupied by a subchain, designated by "$2R$" in Figure 1, is considered as a cylinder, a cube, or a sphere, where k_B, T, and η are Boltzmann's constant, the absolutely temperature, and the solvent viscosity, respectively. The quantitative comparisons below take the small confined space as a cylinder because this physically reasonable choice corresponds more closely to the real situation inside the tube.

We have experimentally confirmed the existence of a critical flow rate for the passage of linear chains through a small cylindrical pore and of the first-order coil-to-stretch transition.[1] However, our measured q_c decreases as the pore size increases,[2] and the measured values under various experimental conditions are 10^2-10^3 times smaller than those predicted using the blob model.[10] To explain these discrepancies, we have again considered the full draining limit in which each subchain inside the pore is characterized by an effective subchain length (L_e) along the direction of the elongation flow. Using a scaling argument relating the pore diameter (D) and the number of Kuhn segments (N) per subchain, i.e., $D = kN^\alpha$, we have derived[2]

$$q_c = \frac{k_BT}{12\eta}\left(\frac{D}{L_e}\right) = \frac{k_BT}{12\eta}\frac{\sqrt{3}k^{1/\alpha}D^{1-1/\alpha}}{l} \qquad (1)$$
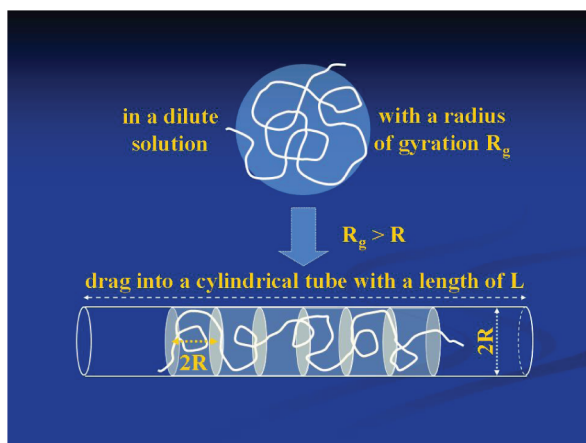
Figure 1. Schematic representation of a linear chain in a dilute solution before and after being dragged into a long cylindrical tube with a radius smaller than its radius of gyration.

where $k_BT/12\eta$ is the critical flow rate $(q_{c,HS})$ when each subchain (blob) is treated as a hard sphere, l is the Kuhn length, $L_e = lN/\sqrt{3}$, k is a constant that is proportional to l, and $0.5 \leq \alpha \leq 0.6$ with the lower and upper limits, respectively, for theta and good solvents. Equation 1 enables qualitatively explaining why the observed q_c are much smaller than those predicted by the hard-sphere blob model and why they decrease with increasing the pore size.

Recently, Freed[12] has applied his Laplace–Green's function/numerical inverse Laplace transform methods to evaluate quantitatively the confinement free energy and drag force for the flow of linear (theta solution) chains through a cylindrical tube whose length far exceeds that of the chain and whose walls present the whole range of interactions (including repulsive and attractive boundary conditions). The evaluation of the drag force exhibits remarkable advantages of the Laplace–Green's function methods over the traditional eigenfunction expansion schemes, especially for general interactions between the chain and the tube walls. The more cumbersome traditional methods would require (a) the numerical solution of a transcendental equation to enable introduction of the eigenfunctions, (b) the introduction of doubly infinite expansions in eigenfunctions for the general case, and (c) the numerical evaluation of the radial integral for each term in the sums, integrals in the series expansions that depend on the eigenvalues from the transcendental equations. The Laplace–Green's function approach, in contrast, requires only a numerical inverse transform of a closed form analytical expression and is, therefore, far more efficient than the traditional methods, especially (1) in the intermediate range wherein the chain and the pore are of comparable sizes and (2) for the practically important,[13] but mathematically rather challenging, systems with finite, nonzero polymer–pore wall interactions.

In order to invoke the free draining limit, Freed and Wu consider a chain segment ("blob") with N Kuhn segments and an effective length L_e along the tube which thus occupies a volume of $V = 2\pi R_g{}^3$. The average segment concentration $c = N/V \sim c^*$, the chain overlap concentration, where polymer dynamics are closer to those predicted by a Rouse, free draining model than a Zimm, nondraining model because solvent molecules are forced to flow through the tube and each confined subchain must be draining. Since analytical calculations with partially screened hydrodynamics are not possible for the cylindrical geometry, the following comparison of their theory with experiment serves as a stringent test of this assumption.

The theoretical calculations of Freed and Wu[12] enable the quantitative determination, *without adjustable parameters*, of the critical flow rate (q_c) for an elongation flow to begin permitting a linear polymer chain in a theta solution to pass through a small cylindrical tube. To define the notation and facilitate the discussion, a brief review of some key equations from ref 12 is required. The chain is immersed in a Poiseuille flow of a fluid with viscosity η and pressure drop of $\Delta P/\Delta x$ per unit length. The total drag force (F_h) on the chain in the free draining limit is the average of the fluid velocity $v(r)$ over the chain conformations, integrated over all the Kuhn segments in the chain, namely

$$F_h = -\zeta \int_0^N d\tau \, \langle v[\mathbf{r}(\tau)] \rangle \tag{2}$$

where $\mathbf{r}(\tau)$ represents the continuous chain conformation of the confined chain segments and $\zeta = 3\pi\eta l$ is the friction coefficient of individual Kuhn segments. The Poiseuille flow implies that the fluid velocity in the cylinder has the profile

$$v(r) = -\frac{4}{\eta}\frac{\Delta P}{\Delta x}(R^2 - r^2) \tag{3}$$

Let $\rho(r,N,c)$ denote the average chain density at the radial distance (r) from the tube center, whereupon the Laplace transform of F_h in the free draining limit can be written as

$$F_h(N,c,R) = -\zeta \mathscr{L}^{-1}\left\{\int_0^R 2\pi r v(r)\rho(E,c,r) \, dr\right\} \tag{4}$$

where $\rho(E,c,r) = \int dN \exp(-EN)\rho(E,c,r)$ and $\mathscr{L}^{-1}$ denotes the inverse Laplace transform. The ability of deriving a closed form expression for the integral in braces critically facilitates evaluating the numerical inverse Laplace transform for arbitrary polymer–surface interaction parameters $(c$, the dimensionless interaction energy per unit length). When $c < 0$, the tube surface is repulsive, while $c > 0$ describes attractive walls. The chain partition function $Z_{confine}$ is evaluated from the chain distribution Green function $G(\mathbf{r},\mathbf{r}';N,c,R)$ by

$$Z_{confine}(N,c,R) = \exp(-A_c/k_BT)$$

$$= \iint d\mathbf{r} \, d\mathbf{r}' \, G(\mathbf{r},\mathbf{r}';N,c,R) \tag{5}$$

where A_c is the free energy of confinement and the integral is over the volume inside the cylinder. The Laplace transform of the chain density $\rho(\mathbf{r};E,c,R)$ is evaluated from $G(\mathbf{r},\mathbf{r}';E,c,R)$ as

$$\rho(\mathbf{r};E,c,R)Z_{confine}(N,c,R)$$

$$= \iint d\mathbf{r}' \, d\mathbf{r}'' \, G(\mathbf{r}',\mathbf{r};E,c,R)G(\mathbf{r},\mathbf{r}'';E,c,R) \tag{6}$$

The Laplace transform of the confinement partition function and the right-hand side of eq 6 are both evaluated analytically.

Figure 2 exhibits the calculated confinement free energy for $cR = -1000$. Actually, when $cR = -20$, the surface is already sufficiently repulsive that it may be treated as a completely repulsive surface.[12] A fit to the data in Figure 2 yields

$$A_c \approx k_BT\left[1.05 + 5.78\left(\frac{R_g}{R}\right)^2\right] \tag{7}$$

Figure 1 suggests that the chain inside the tube may be decomposed into a series of subchains, each of which occupies a small cylindrical space. Because the subchains are statistically
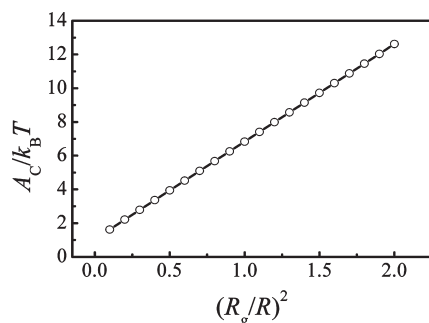
Figure 2. Dependence of confinement energy (normalized by the thermal energy) on relative chain size, where the line presents the least-squares fit to data.

equivalent, A_c equals the product of the confinement free energy of each subchain and the number of subchains. In other words, we only need to consider the first subchain that enters the tube and may ignore the chain length as long as the chain is much shorter than the tube length. This assumption physically means that the flow is critical and that it is only necessary to drag or push the first subchain into the tube because the rest of the chain simply follows the strong flow. Each subchain has the size $R_g \sim R$, so that the confinement force (f_c) on each subchain is

$$f_c = \frac{A_c}{V_{cylinder}} \pi R^2 = \frac{3.42 k_B T}{R} \qquad (8)$$

where $A_c/V_{cylinder}$ is the osmotic pressure generated by the subchain inside the tube and $V_{cylinder}$ is the small volume occupied by each subchain. Further, the evaluation of the integrals in eq 6 leads to $\rho(r;E,c,R) Z_{confine}(N,c,R)$ that has been inserted into eq 4 to yield the hydrodynamic drag force as[12]

$$F_h = \frac{4}{\eta} \zeta \frac{\Delta P}{\Delta x} \frac{R^4 N}{R_g{}^2} F_{red}(N, cR) = \frac{24\zeta R^4}{\eta l^2} \frac{\Delta P}{\Delta x} F_{red}(N, cR) \qquad (9)$$

where $R_g{}^2 = N l^2/6$ for a Gaussian chain, $\Delta P/\Delta x$ is related to the flow rate (q) in classic fluid mechanics as $q = (\pi R^4/8\eta)(|\Delta P/\Delta x|)$, and $F_{red}(N,cR)$ is a reduced dimensionless function. Note that q is used to denote the flow rate instead of J in ref 12 to be consistent with the notation in refs 1–5. In the limit of a completely repulsive surface ($cR \rightarrow -\infty$),[12] the theory yields

$$F_{red}(N, cR) \cong 0.741 \left(\frac{R_g}{R}\right)^2 + 0.010 \left(\frac{R_g}{R}\right)^4$$

$$(\text{for } (R_g/R)^2 > \sim 0.7) \qquad (10)$$

while for a less repulsive surface, $F_{red}(N,cR)$ can drop $\sim$15% as cR ranges from -20 to -2 for $R_g = R$. The combination of eqs 9 and 10 leads to

$$F_h \cong \frac{192\zeta}{\pi l^2} q \left[0.741 \left(\frac{R_g}{R}\right)^2 + 0.010 \left(\frac{R_g}{R}\right)^4\right] \qquad (11)$$

Following similar arguments, F_h equals the product of the hydrodynamic force experienced per subchain (f_h) and the
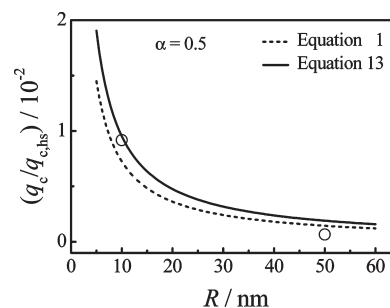
Figure 3. Dependence of calculated normalized critical flow rates (q_c and $q_{c,HS}$) on tube radius, where $q_{c,HS} = k_B T/12\eta$ and the two circles represent measured values for polystyrene in cyclohexane at 34.3 °C (ref 3).

number of subchains. Since each subchain is characterized by $R_g \sim R$

$$f_h \cong \frac{144\zeta}{\pi l^2} q \qquad (12)$$

Therefore, by increasing q, the critical flow rate (q_c) at which $f_h = f_c$ emerges as

$$q_c = q_{c,HS} \frac{l}{10.5 R} \qquad (13)$$

where $q_{c,HS} = k_B T/12\eta$ is the hard-sphere approximation that involves treating each subchain as a randomly moving hard sphere inside a small cylinder $[\pi R^2(2R)]$,[10] $l \sim 1$ nm for typical linear flexible polymer chains, and R is in units of nm. Equation 13 qualitatively supports our previous scaling argument summarized in eq 1; i.e., q_c is inversely proportional to R in theta solutions ($\alpha = 0.5$).

Figure 3 demonstrates that the two measured values of $q_c/q_{c,HS} = 9.17 \times 10^{-3}$ and 6.55×10^{-4} (ref 3) are close to those calculated from eq 13 *without adjustable parameters* and to those from eq 1 using the previous experimentally determined scaling relationship,[14] $\langle R_g \rangle$ (nm) $= 2.82 \times 10^{-2} M_w{}^{0.5}$. Surprisingly, our previous simple scaling argument embodied in eq 1 accords with the current more quantitative analysis (eq 13) for polymers in theta solutions. The overall agreement between the measured and calculated critical flow rates is rather satisfactory considering all the uncertainties in the measured values, especially for the large pore with $R = 50$ nm. Moreover, eq 1 additionally predicts that q_c increases as the solvent quality improves, i.e., as α increases.

Figure 4 displays how the measured ratio $q_c/q_{c,HS}$ for linear polystyrene chains in cyclohexane varies with the solution temperature.[3] Most prior studies determine the theta temperature for polystyrene in cyclohexane as $\sim$34.5 °C from the vanishing of the second virial coefficient. The calculated and measured values of $q_c/q_{c,HS}$ near $\sim$34.5 °C in Figures 3 and 4 are in reasonably good agreement. The comparison demonstrates that both the current rigorous evaluation (using a combination of the Laplace–Green's function methods and numerical inverse Laplace transforms of closed form analytical expressions) and our previous rough estimation using a simple scaling argument are sufficient for quantitatively describing how a linear polymer chain in a dilute solution passes through a small cylindrical tube ("nanopore").

Note that Figure 4 reveals a minimum in q_c around 35 °C, which can be qualitatively attributed to a balance between changes of enthalpy and entropy under theta conditions; namely, the chain becomes the most deformable at this point. The elevation
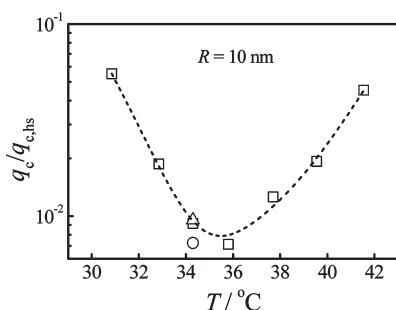
Figure 4. Measured temperature dependence of the normalized critical flow rate ($q_c/q_{c,HS}$) for polystyrene in cyclohexane (ref 3), where $q_{c,HS} = k_B T/12\eta$ and the circles and triangles represent the two calculated values from eqs 1 and 13, respectively.

of q_c with increasing solution temperature on the right side of the minimum is due to chain swelling in good solvents; namely, a higher hydrodynamic force (a faster flow) is required in order to squeeze and stretch a swollen polymer chain and thereby increase its entropy. Equations 2 and 5 provide the expectation that both F_h and F_c would decrease in good solvents because each confined subchain has a smaller number N of Kuhn segments. The increase of q_c on the right side of Figure 4 indicates that F_h must decrease faster than F_c as the chain swells, so that a higher flow rate is required to obtain the force balance $F_h = F_c$.

On the other hand, the increase of q_c with decreasing solution temperature on the left side of Figure 4 should be related to the stronger chain segment–segment attraction in poor solvents; i.e., the flow has to be faster in order to override the extra enthalpic force resisting the stretching of the chain. As the solution temperature decreases, the chain gradually shrinks, so that each subchain inside the tube becomes less draining and has diminished confinement energy. The increase of q_c with descending solution temperature in Figure 4 suggests that the draining effect begins to overpower the confinement in poor solutions. The quantitative evaluation of the hydrodynamic force and confinement energy in good solvents are rather challenging, but in poor solvents, the quantitative evaluation of how linear chains are confined inside a cylindrical tube and are stretched under an elongation flow becomes even tougher to handle.

In summary, satisfactory agreement is obtained between the calculated and measured critical flow rates (q_c) of elongational flow for linear polystyrene chains in theta solutions to pass through a small cylindrical tube ("nanopore") of radius smaller than the chain size. This agreement demonstrates the validity of our previous derivations of the hydrodynamic force and confinement energy of a linear chain inside a cylindrical tube. The theories satisfactorily explain why the measured values of q_c are 10^2-10^3 lower than those predicted by de Gennes[10] using a hard-sphere, "blob" model for each subchain inside the tube, and they further predict that q_c is inversely proportional to the tube radius, unlike the tube radius independence of the hard-sphere model. The Laplace–Green's function methods are tractable for different interacting tube walls and are extendable to star chains and other chain topologies. On the other hand, our prior scaling argument can predict the dependence of q_c on solvent quality. The extension of our rigorous evaluation to polymer chains in good solvents is under consideration. As expected, the average local concentration decreases in good solvents; each confined subchain should be more draining to solvent molecules that are forced through the tube. The next real challenge of the theories is to describe the behavior in poor solvents.

■ AUTHOR INFORMATION

Corresponding Author

*E-mail: freed@uchicago.edu (K.F.F.); chiwu@cuhk.edu.hk (C.W.).

■ REFERENCES

(1) Jin, F.; Wu, C. *Phys. Rev. Lett.* **2006**, *96*, 237801. *Acta Polym. Sin.* **2005**, *4*, 486.

(2) Ge, H.; Pispas, S.; Wu, C. *Polym. Chem.* **2011**, *2*, 1071.

(3) Ge, H.; Jin, F.; Li, J. F.; Wu, C. *Macromolecules* **2009**, *42*, 4400.

(4) Hong, L. Z.; Jin, F.; Li, J. F.; Lu, Y. J.; Wu, C. *Macromolecules* **2008**, *41*, 8220.

(5) Ge, H.; Wu, C. *Macromolecules* **2010**, *43*, 8711.

(6) Casassa, E. F.; Tagami, Y. *Macromolecules* **1969**, *2*, 14.

(7) Edwards, S. F.; Freed, K. F. *J. Phys. A (London)* **1969**, *2*, 145.

(8) Carslaw, H. S.; Jaeger, J. C. *Conduction of Heat in Solids*; Clarendon Press: Oxford, 1984.

(9) Rouse, P. E. *J. Chem. Phys.* **1953**, *21*, 1272.

(10) de Gennes, P. G. *J. Chem. Phys.* **1974**, *60*, 5030.

(11) Pincus, P. *Macromolecules* **1976**, *9*, 386.

(12) Freed, K.; Wu, C. *J. Chem. Phys.* **2011**, *135*, 144902.

(13) Mueller, M.; Steinmueller, B.; Daoulas, K. C.; Ramirez-Hernandez, A.; de Pablo, J. *J. Chem. Phys. Phys. Chem.* **2011**, *13*, 10491.

(14) Appelt, B.; Meyerhoff, G. *Macromolecules* **1980**, *13*, 657.